Nonlinear Dyn (2024) 112:20661–20676
https://doi.org/10.1007/s11071-024-10058-3

RESEARCH

Reaching a desirable metastructure for passive vibration attenuation by using a machine learning approach

Ivana Kovacic · Zeljko Kanovic · Vladimir Rajs · Ljiljana Teofanov · Rui Zhu

Received: 28 April 2024 / Accepted: 20 July 2024 / Published online: 26 August 2024

Abstract The focus of this research is on designing a longitudinally excited lightweight metastructure that consists of external units distributed periodically, each enhanced with internal oscillators to serve as vibration absorbers. The metastructure initially exhibits uniformity, with all absorbers being identical to each other, being comprised of a cantilever that is integrated into the external parts of the metastructure, with each cantilever containing a concentrated mass block at its tip. Despite its simplicity and suitability for 3D printing, the design of the absorbers could not be kept in the original form when previous theoretical attempts were made with a view to achieving maximal vibration attenuation efficiency around the second resonance. To overcome this shortcoming and keep the absorbers in the original shape, this study undertakes a machine learning methodology to mitigate vibrations near the second resonant frequencies itself, as well as around the first and second resonant frequencies simultaneously. The newly designed metastructure is manufactured, and its advantageous vibration mitigation capabilities are experimentally verified qualitatively. Additionally, physical insight into the configuration and arrangement of the redesigned absorbers in the newly designed metastructure is provided.

Keywords Metastructure · Vibration attenuation · Absorbers · Design · Machine learning

I. Kovacic (✉)
Faculty of Technical Sciences, Centre of Excellence for Vibro-Acoustic Systems and Signal Processing CEVAS, University of Novi Sad, Novi Sad, Serbia
e-mail: ivanakov@uns.ac.rs

Z. Kanovic · V. Rajs · L. Teofanov
Faculty of Technical Sciences, University of Novi Sad, Novi Sad, Serbia

R. Zhu
School of Aerospace Engineering, Beijing Institute of Technology, Beijing 100081, China

1 Introduction

The concept of ‘metastructures’ has recently emerged in the field of vibration control, drawing inspiration from the development of metamaterials [1–3]. This approach involves utilizing an array of distributed and appropriately tuned auxiliary oscillators, usually positioned within/on the external/main components of a structure to effectively manage its vibration response. While the term itself is relatively new, its essence can be traced back to the extension of Den Hartog’s methodology [4] for controlling the response of a main vibrating structure, which is modelled as a one-degree-of-freedom linear mechanical oscillator. This extension entails incorporating an auxiliary oscillator in a manner that aligns (tunes) the frequencies of the main structure, the external harmonic excitation, and the auxiliary oscillator. Thus, the auxiliary oscillator

should be carefully designed from the viewpoint of its natural frequency. This ensures that instead of resonating infinitely at this specific frequency, the externally excited undamped main structure will undergo antiresonance, resulting in a zero-displacement amplitude [4–6]. The auxiliary oscillator works as a vibration absorber, also known as a tuned-mass-damper in the presence of damping [7, 8]. While tuning auxiliary oscillators in diverse types of oscillators to target their resonances has gained significant interest in the vibration community [9–12], the same level of attention has not been given to their particular tuning in metastructures. There are several factors contributing to this phenomenon. Firstly, there is a wide range of mechanical models for metastructures and a unified approach that encompasses all these models has not yet been established. Secondly, metastructures derived from metamaterials are often represented as chains of numerous mass-in-mass units. This complex configuration makes it challenging to analytically solve the system of the corresponding governing equations. As a result, researchers have turned to numerical methods. Considering the focus of the current study on longitudinal vibrations, a chronological overview of some of the numerical approaches employed so far, and the corresponding outcomes are provided solely for these vibrations. Thus, in [13], a slender beam containing periodically attached oscillators was examined. Through both theoretical analyses using the transfer matrix method and experimental observations, it was discovered that a highly asymmetric attenuation occurred within a subfrequency locally resonant bandgap. The key parameters that affect the attenuation in the bandgap were identified as the stiffness and mass ratios. Results from another study [14] showed that discrete models of a unit cell, developed using integration and finite difference methods, were suitable only for elastic waves with wavelengths significantly longer than the unit cell's length. Furthermore, finite-element simulations demonstrated that a metamaterial-based absorber shared similarities with traditional mechanical vibration absorbers, as discussed earlier. The design of a broadband absorber was expanded upon by implementing this approach, and the effectiveness of the design was confirmed through numerical illustrations. The research discussed in [15] focused on uniform rods containing a periodic arrangement of resonators. The numerical findings indicated the presence of both Bragg-type and resonance-type bandgaps within this system, demonstrating the possibility of achieving multiple desired resonance gaps. The impact of resonator parameters on bandgap characteristics, including location, width, and attenuation performance, was analysed by generating plots of the attenuation constant surfaces. The research presented in [16] introduced analytical and finite element modelling techniques for a 3D-printed metastructure featuring 10 absorbers, which was subsequently produced and examined experimentally. The experimental results revealed that the frequency response of the metastructure prototype matched the predicted response, effectively eliminating vibration at the specified design frequency and suppressing vibration across a frequency range of up to 275 Hz. The investigation conducted in [17] focused on metamaterial rods with resonators attached periodically, which were analysed using a numerical approach combining Finite-Element Modelling (FEM) and Floquet–Bloch's theorem, as well as the commercial finite element software ANSYS. An intriguing characteristic observed in the rod under consideration is that before the bandgap, the vibration response of the system exhibits low damping, while after the bandgap, it demonstrates a high damping vibration response. The study outlined in [18] demonstrated the practicality of utilizing distributed vibration absorbers in a metastructure to mitigate its response without adding any extra mass to the system. The simulations showed that the distributed absorbers must satisfy particular requirements, which encompass possessing natural frequencies within a wide spectrum of frequencies, a mass ratio of absorbers to host structure around 0.30, with approximately 20 absorbers whose natural frequencies vary linearly across the structure. In [19], a comprehensive theory was presented for estimating bandgaps in 1D or 2D vibrating structures using a differential operator approach. By assuming an infinite number of resonators of the structure, all tuned to the same frequency, a straightforward expression for the edge frequencies of the infinite-resonator bandgap was established. This expression was found to be dependent on the ratio of the additional mass and the target frequency. The study demonstrated that locally resonant bandgaps can be induced in nonuniform structures as long as the masses of the resonators are distributed in proportion to the mass distribution of the primary structure. Furthermore, it was determined

that a minimum quantity of resonators is necessary for the bandgap to manifest, and that there exists an optimal number of resonators for achieving the widest possible bandgap. Through numerical investigations, it was concluded that the width of the bandgap diminishes with variations in the resonant frequencies of the resonators, although some degree of variation can be accommodated depending on the number of resonators and the modal vicinity of the bandgap. Furthermore, the absence of a requirement for periodicity in the placement of resonators was discovered, as the creation of a bandgap is possible through the utilization of nonuniform spatial distributions of resonators. In [20], a discrete mechanism was introduced to reduce longitudinal vibrations in a low frequency range, showing the effectiveness of vibration mitigation using both computational and experimental methods. The impact of unit cell parameters on the upper limit frequency of the stopband was also examined. This theoretical approach was further expanded to encompass a continuous system, which holds significant practical implications.

The utilization of data science and, machine learning (ML) accordingly, has undeniably expanded the possibilities in the numerical development and adjustment of engineering structures. However, this particular approach has not been extensively utilized in the creation of metastructures that possess desirable vibration control properties with specifically adjusted or tuned auxiliary oscillators. In [21], an Archimedean spiral metastructure was proposed for the purpose of controlling low-frequency flexural waves. Its inverse design, focusing on the desired bandgap width and central frequency, was achieved through employment of the ML method. The validity of this approach was confirmed through both FEM and experimental testing. The study presented in [22] employed numerical simulations and ML techniques to conduct both forward and inverse design strategies for a composite metastructure, aiming to achieve subwavelength and ultrawide bandgaps. The ML results were validated through numerical analysis as well as experimental testing on fabricated 3D-printed structures, with separate excitations applied in the longitudinal and transverse directions. To obtain an optimal model of a metastructure that takes into account both structural safety and quasi-zero stiffness characteristics, a combination of deep reinforcement learning, and FEM has recently been utilized within an optimization framework [23]. The 3D printing is then employed, and the experiments demonstrated that the fabricated metastructures exhibit remarkable performance in reducing vibrations, even in the low-frequency range. The achievement of notable isolation characteristics for low-frequency flexural vibrations was observed in hull grillage metastructures [24] as well. The dataset was created by employing the wave mechanics theoretical model of hull grillage metastructures, and subsequently, the forward prediction neural network model was utilized to determine the vibration transmission characteristics. In [25], a phononic crystal-based metastructure was considered, and a novel deep learn-based technique was introduced to enable its optimization using qualitative and quantitative descriptions, thus minimizing the risk of misjudgements. Additionally, the optimization process included metastructures with varying periodic constants and filling fractions, providing valuable insights into achieving a balance between space, material utilization, and vibration isolation. The effectiveness of the optimized designs in terms of vibration performance was confirmed through the utilization of FEM. A recent paper on the utilization of ML in the field of nonlinear dynamics [26] pointed out that ‘A challenge in these problems is the high dimensionality of the design parameter spaces, but …, this can be addressed through tools of machine learning, which can, not only provide predictions of designs of high performance, but also can inform studies of robustness of such solutions’. The recent review paper on ML- assisted intelligent design of metastructures [27] stated that ‘ML can theoretically provide excellent design results for various acoustic or mechanical requirements of targets, but most current research lacks manufacturing and experimental verification after design’.

The main objective of the present study is to expand the potential of the use of data science and ML in particular, in the field of vibration control for metastructures. The study also aims to validate the design qualitatively through manufacturing and experimental investigations, contributing to the shortcomings highlighted in the quotation above from the review article [27]. There is an important specific objective as well, and it regards the previous limitations of theoretical investigations presented in [28]. Namely, these theoretical results led to the conclusions that the specifically tuned absorbers could not be kept in the original shape but needed to be changed so as to achieve

vibration attenuation around the second resonance because of the associated stiffness requirements. However, for practical reasons, it can be desirable to keep the shape of the absorbers as in the original form but just change their dimensions, and the current study employs a ML approach to accomplish this specific objective and to optimize the design of internal auxiliary oscillators in this manner.

The overview of this study is as follows. The original structure and its variations are detailed in Sect. 2. The ML procedure and the outcomes obtained are explained in Sect. 3. In Sect. 4, the vibration response of the newly designed metastructure, are validated qualitatively via detailed numerical results as well as experimentally. Section 5 provides an analytical analysis of the shape and distribution of the internal oscillators in the redesigned metastructure. Finally, Sect. 6 summarizes the findings and presents the corresponding conclusions.

2 Basic model and its variations

2.1 On the basic model

The primary metastructure being examined, which is referred to as MS0, is comprised of external units and internal oscillators. This metastructure is initially defined in [16] and is represented in Fig. 1a. The external unit possesses a hollow square cross-section, with its fundamental characteristics denoted in Fig. 1a as well. Specifically, the external width and length are identified as a, the length of the walls is denoted as u, and the height of the transversal elements (i.e., the floor and the ceiling) is labelled as r.

The internal oscillator illustrated in Fig. 1a comprises a cantilever with dimensions denoted as length L and height e, featuring a concentrated mass at its tip forming a discrete block. The specific dimensions of the internal oscillator, including length d, width a, and height b, can be seen in Fig. 1a. Throughout subsequent discussions, this integrated system will be referred to as the absorber type TA0. The internal oscillator is symmetrically incorporated into the wall of the external unit at a designated position determined by parameter p relative to the ceiling and the floor. In Fig. 1b, a unified 10-unit metastructure is shown, which is obtained by multiplying the combined units, excluding the floors. Each unit and absorber within the metastructure are assigned a number from 1 to 10, starting from the bottom. The detailed geometric parameters are provided in Table 1. To mitigate bending, pairs of internal oscillators are attached to

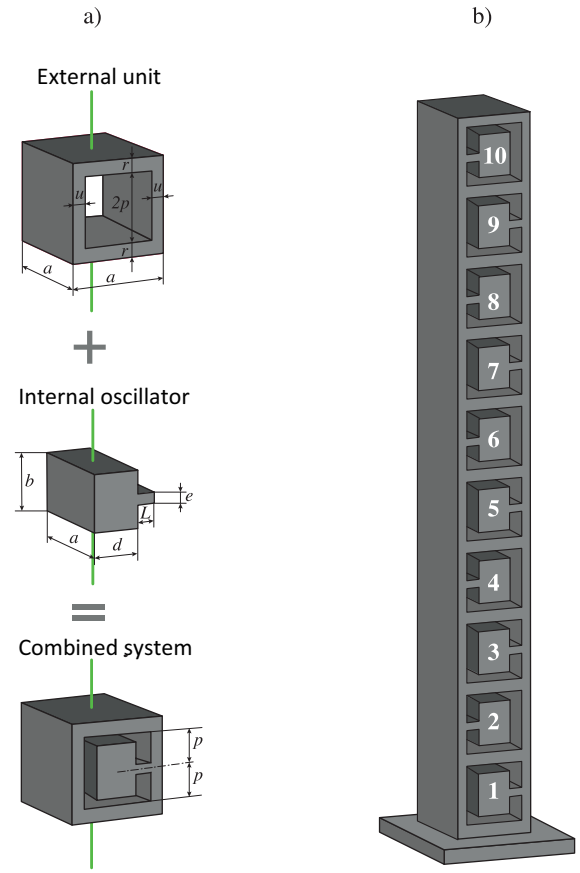

Fig. 1 **a** Parameters of the external unit, the internal oscillator and the combined system; **b** Basic metastructure MS0 with external units and 10 internal oscillators, labelled 1–10

Table 1 Parameters of MS0

Part	Parameter	Value [mm]
External unit	u	6.5
	r	6.5
	p	14
Internal oscillator	L	6.5
	e	4
	d	17
	b	20
External unit & internal oscillator	a	40

the opposing internal walls of the external units, as depicted in Fig. 1b. The odd-numbered oscillators are fixed to one side of the wall of the external units, while the even-numbered oscillators are attached to the opposite side.

The idea to be used is that internal oscillators perform transversal oscillations whose direction is aligned with the direction of longitudinal oscillations of each unit and the metastructure as a whole, as indicated by the green solid line in Fig. 1a. This metastructure has been shown to be appropriate for manufacturing via 3D printing as it is homogenous and uniform, and, thus, suitable to be extended to a desirable number of units while achieving a good vibration attenuation around the first resonance [28]. However, the design of absorbers is a topic that needs further exploration, especially when it comes to attaining the highest possible efficiency in vibration attenuation around the second resonance region, as well as around the first and second resonant frequencies simultaneously but keeping them in the same shape. So, the question is if all of them should be equal mutually or if their dimensions and distribution should vary along the metastructure. The following considerations aim to answer this question.

2.2 On the variations

The redesign of the basic metastructure is done while focusing on the internal oscillators, affecting the lengths of the mass block and the cantilever, i.e. parameters d and L. However, to keep the longitudinal axis of the metastructure fixed and prevent bending from happening, the sum of these lengths needs to satisfy the following constraint $L + d/2 = \text{const.}$, which represents the first physics-based condition taken into account so that the structure keeps the same vertical symmetry axis. Further, the value of the parameter d is taken in three versions: the one in MS0 is treated as the zero-variation, the next value of d corresponds to the half of the original one, and the third value of d is equal to zero, when there is no block mass located at the end of the cantilever.

To avoid further bending, the second physics-based criterion for redesign involves altering internal oscillators 1–10 in pairs. The assumption is that each consecutive pair must be geometrically equivalent: $1 = 2$, $3 = 4$, $5 = 6$, $7 = 8$, $9 = 10$. Consequently, there will be a total of five pairs of internal oscillators requiring redesign. By considering three different variations of parameter d across these five pairs, a total of $3^5 = 243$ distinct metastructures will be initially considered, as explained in the following section in detail.

3 Redesign via metastructure model-informed machine learning approach

The workflow of the redesigning procedure is described symbolically in Fig. 2. It consists of the following three steps, which also define a general procedure on how to construct the ML problem for the vibration control of metastructures:

- Step 1: Utilize simulation software with coupled modelling capabilities (geometrical and physical) and results evaluation to perform an in-depth numerical vibration analysis of all variations of the metastructures. This utilization should generate a dataset that captures the amplitude-frequency response curves (AFRCs) of the point located at the top of each metastructure;
- Step 2: By employing the discrete numerical dataset from Step 1, undertake ML techniques to obtain the continuous metastructure model as a basis for absorber geometry optimization. Consider more ML techniques and choose the one providing the most accurate model;
- Step 3: Using the continuous ML model obtained in Step 2, conduct the optimization process, with the objective to establish the most suitable geometry of the absorbers, focusing primarily on maximizing the width of the desirable vibration attenuation region(s).

The details of this procedure applied to the metastructure under consideration are given below.

While performing Step 1, all 243 variations of the metastructure defined in the last paragraph of Sect. 2.2. are generated in Excel, maintaining a fixed shape and geometry of the external units but allowing for changeable geometry of the internal units. These variations are presented in a colourful Excel table on the left side of Fig. 2 in Step 1. The table used includes all the variations along with their respective parameter values. Subsequently, these variations are imported into the software COMSOL Multiphysics, where the corresponding metastructures are then visualized

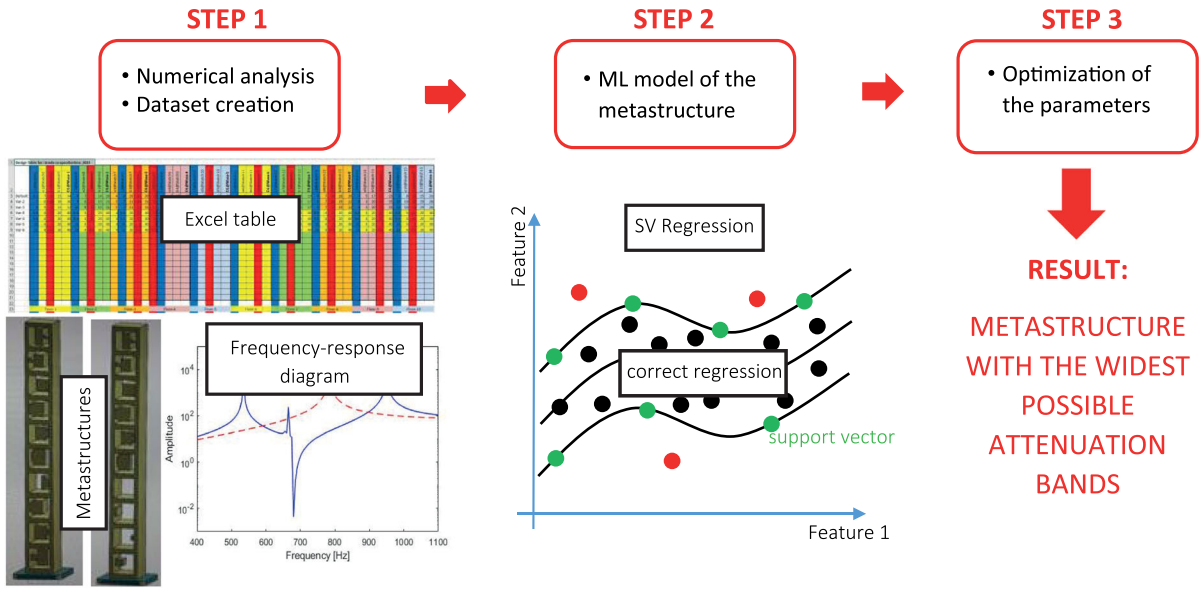

Fig. 2 Workflow of the redesign procedure with an overview of the methodologies used

based on the geometrical parameters imported. As an example, two of these metastructures are displayed in the lower left corner of Fig. 2. For the internal oscillator, the numerical values for a cantilever of lengths 6.5 cm, 10 cm, and 15 cm are considered (note that this is related to the first physics-based criterion of keeping the vertical axis fixed discussed earlier, causing the change both in the parameters d and L). Further, to closely match the subsequent numerical results with the fabricated metastructures, the material properties are set as follows: a Young's modulus of elasticity $E = 1900$ MN/m^2 and a density $\rho = 1.015$ g/cm^3 (these values are obtained from the manufacturer for the metastructures produced and experimentally examined, see Sect. 4). Subsequently, the AFRCs of the point situated atop the metastructure are acquired for each variation. An illustration of one such frequency–response diagram can be seen in the lower left section of Fig. 2.

In Step 2, the obtained data and diagrams are used to calculate the width of the vibration attenuation regions around the second modal frequency. The attenuation region is defined as the frequency region in which the displacement amplitude of the new metastructure is lower than the displacement amplitude of MS0, as also defined in [28]. The acquired geometric information and the calculated width of the attenuation regions are then utilized to construct a mathematical model of the metastructure using ML techniques. Two specific ML techniques, namely and Support Vector Regression (SVR) [29] and Artificial Neural Networks (ANN) [30] are taken into consideration. In both approaches, the obtained numerical dataset is employed to train the metastructure model. This involves utilizing various combinations of continuous geometric parameters for different metastructure variations as input data, while the corresponding attenuation region width is used as the output data. The total number of inputs is 10, corresponding to the values of L and d for each pair of internal oscillators in the metastructure, while the number of outputs is two, associated with two attenuation regions—around the first and second modal frequency. Although this interpretation of the model contains redundant inputs /features, since the constraint $L + d/2 = \text{const.}$ must be satisfied, this form is adopted for more clear understanding of the input features. In general, the model with redundant features is not less accurate, it is just not optimal regarding the size and efficiency, so the suggested model architecture does not affect the quality of the results. The performance and accuracy of both ML models derived in this manner were assessed using Root Mean Square Error (RMSE) and Mean Absolute Error (MAE) values. Both these criteria are often used to describe the accuracy of the ML model with respect to known target data. RMSE is

defined as $\left[\sum_{i=1}^{N}(f_i - t_i)^2/N\right]^{1/2}$, where f_i and t_i stand for forecasted and target values respectively, and N is the number of samples. On the other hand, MAE is defined as $\left(\sum_{i=1}^{N}|f_i - t_i|\right)/N$. For the ANN model, the RMSE value was 13.598 and the MAE was 6.421. The architecture of this model was determined through a trial-and-error process, with the network comprising one hidden layer with 13 neurons. In the case of the SVR model, the RMSE value was 9.547 and the MAE was 4.236. The model with a cubic kernel was selected, surpassing other kernel variants examined (linear, quadratic, fine, medium- and coarse-Gaussian). Based on these findings, one can conclude that the SVR model with the cubic kernel outperforms the ANN model regarding regression accuracy, so SVR model was chosen as the reference model for further investigation. The central part of Fig. 2, describing the Step 2 of the redesign procedure, depicts SVR model schematically, with its characteristic elements (support vectors holding the margin and the region of accurate regression, presented in 2D feature space).

All the afore-mentioned models were developed, trained, evaluated, and implemented in MATLAB, version R2020b.In Step 3, based on the SVR model of the metastructure, the optimization of the geometrical parameters is conducted. A genetic algorithm is chosen as the optimizer, due to its robustness and ability to find a global optimal solution in the most complicated engineering problems [31]. Two versions of the optimality criterion are proposed:

(i) The width of the frequency region where vibration is reduced around the second resonant frequency and
(ii) the total width of the frequency regions where vibration is reduced around both the first and subsequent (second) resonant frequencies.

It is interesting to note that for both of them, one winning redesigned metastructure is obtained, which is labelled as MS1 hereafter. This metastructure MS1 is shown on the right-hand side of Fig. 3. It is seen that it contains an original design of absorbers, but their distributions are neither intuitive nor expected. Actually, there are three types of absorbers (TA1):

- TA1.1: A cantilever-like absorber with the longest length (absorbers 3, 4, 9, and 10)
- TA1.2: An absorber consisting of a longer cantilever and a shorter tip mass than in TA0 (absorbers 1, 2, 5, and 6)
- TA1.3: An absorber composed of an slightly longer cantilever and a slightly shorter tip mass than in TA0 (absorbers 7 and 8).

The dimensions of these absorbers are given in Table 2.

In what follows, the efficiency of the proposed redesign procedure, regarding time and computational effort, is discussed. Instead of the proposed procedure described above, involving the ML model for the optimization criterion evaluation in a genetic algorithm, the other possible variant of the redesign was to use COMSOL Multiphysics instead of the ML model and combine it with a genetic algorithm, However, each evaluation of a metastructure analysis in COMSOL Multiphysics took averagely 12 min and 2 s, with computation made on Intel Core i7 CPU with 3, 4 GHz speed and 16 GB of RAM. Having in mind that the genetic algorithm needs many model evaluations in each generation, the combination of COMSOL Multiphysics and the genetic algorithm would be highly time-consuming. On the other hand, ML model training and testing in Matlab is time efficient and the calculation time is measured in seconds (averagely 23 s for training and testing). Once the model was created, each evaluation in genetic algorithm took less than a second. These numbers express the true advantage and superiority of the ML model, in the sense of time efficiency and computational efforts needed for the metastructure redesign procedure. Apart from that, COMSOL Multiphysics is not the open-source software and connecting Matlab (for genetic algorithm application) with COMSOL Multiphysics would be a very demanding task, requesting high skills for practical computing implementation.

Figure 3 shows the AFRCs obtained in COMSOL Multiphysics for the top point of the basic metastructure MS0 and the redesigned metastructure MS1, which has been optimized according to criterion (i) and (ii) in the frequency region between 400 and 1100 Hz, which is considered here as a desired frequency band covering two resonances of MS0 of interest in this study. Note that in the subsequent diagrams, the non-dimensional frequency and non-dimensional displacement amplitudes are shown, where the former is calculated as the ratio of the

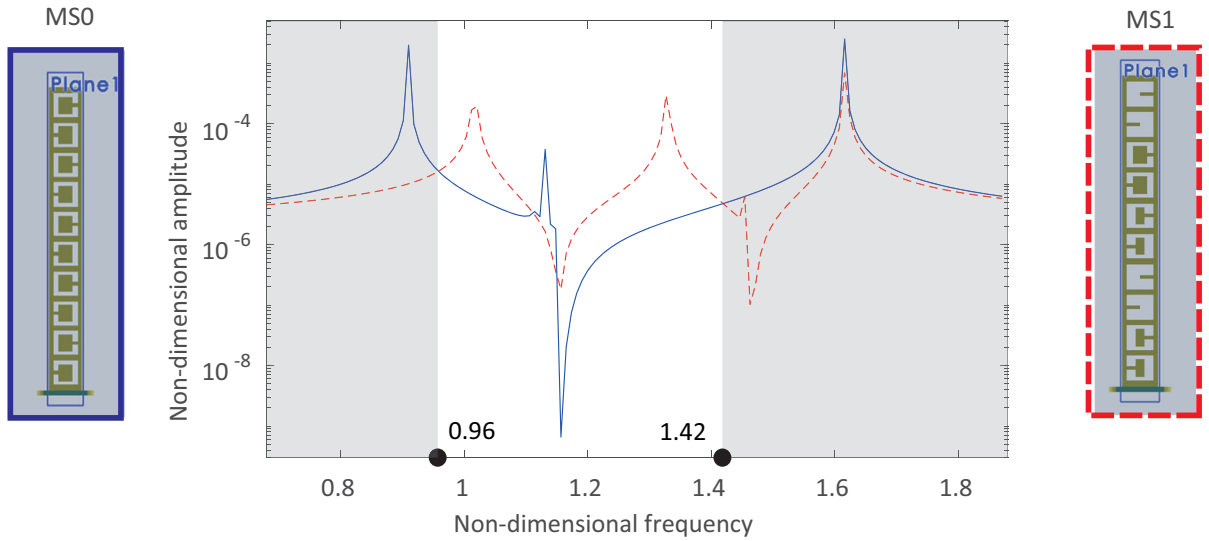

Fig. 3 Numerically predicted AFRCs of the point on the top of MS1 compared to the original one MS0 with the attenuation region shaded in grey

Table 2 Parameters of the metastructure MS1

Parameter of MS1	Internal oscillator number				
	1, 2	3, 4	5, 6	7, 8	9, 10
Types of absorbers (TA1)	TA1.2	TA1.1	TA1.2	TA1.3	TA1.1
L [mm]	9.895	15	9.895	6.6	15
d [mm]	10.21	0	10.21	16.8	0

excitation frequency and the frequency of the MS with blocked absorbers, being 588 Hz [28], while the latter is calculated as the ratio of the displacement amplitude of the top point and the overall height of the MS, being 358 mm. The attenuation region achieved by the MS1 having a small amplitude response then MS0 is shaded in grey seen in this figure (this holds for other subsequent figures, as well). The sketches of both the original metastructure MS0 and the newly redesigned one MS1 are presented on the left and right sides of this figure for the sake of comparison and the definition of legend for the AFRCs shown.

4 Validations

4.1 Numerical validations

To provide more detailed evidence about the reliability of the design of MS1, Table 3 is created, containing 30 configurations out of 243 forms created in COMSOL Multiphysics. All these 30 configurations, labelled herein as MS1.1.-MS1.30, have the same type absorbers T1.1, T1.2 and T1.3 as MS), but they are arranged differently along the MS. So, there are two TA1.1, two TA1.2 and one TA1.3, and they are relocated along the metastructure. For each of them, the quantitative values for the width of the attenuation bands around the first resonance (AB1), the second one (AB2) and their sum (total attenuation band TAB) are also given. It is clearly seen that the winning MS1.15 = MS1 has the widest TAB as well as that just slightly different relocation of the absorber can significantly decrease TAB. It can be seen that MS1.18, for example, has the TAB that is only 62% of the wining one in MS1.15.

4.2 Experimental validation

The original metastructure MS0 as well as the redesigned metastructure MS1 were manufactured using Fused Filament Fabrication technology, which

Table 3 Variations the metastructure MS1 with three types of absorbers distributed differently and the corresponding attenuation bands AB1, AB2 and TAB

Variation	**MS1.1**	**MS1.2**	**MS1.3**	**MS1.4**	**MS1.5**	**MS1.6**
Design	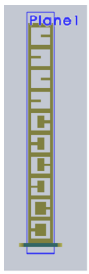			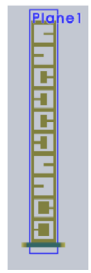		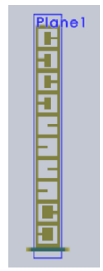
AB1	180.2	178.1	176.3	175.7	174.0	171.6
AB2	154.7	113.4	158.2	169.2	131.7	197.3
TAB	334.9	291.5	334.5	344.9	305.7	368.9
Variation	**MS1.7**	**MS1.8**	**MS1.9**	**MS1.10**	**MS1.11**	**MS1.12**
Design	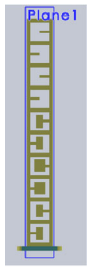			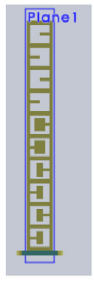	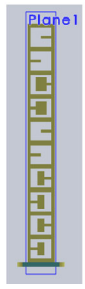	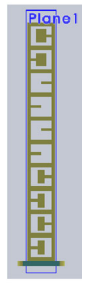
AB1 [Hz]	176.3	174.3	172.7	171.7	165.6	161
AB2 [Hz]	160.0	97.6	110.3	175.8	168.4	164
TAB [Hz]	336.3	271.9	283.0	347.5	334.0	325
Variation	**MS1.13**	**MS1.14**	**MS1.15**	**MS1.16**	**MS1.17**	**MS1.18**
Design	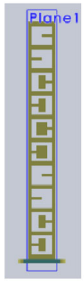					
AB1 [Hz]	167.6	166.1	163.5	159.1	159.8	156.8
AB2 [Hz]	101.7	154.0	265.6	121.6	154.2	109.3
TAB [Hz]	269.3	320.1	429.1	280.7	314.0	266.1

Table 3 continued

Variation	**MS1.19**	**MS1.20**	**MS1.21**	**MS1.22**	**MS1.23**	**MS1.24**
Design	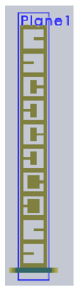	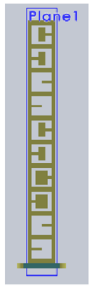	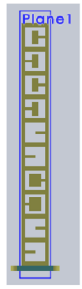	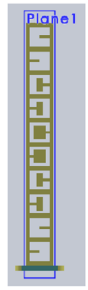	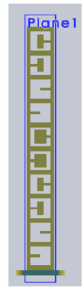	
AB1 [Hz]	170.3	168.8	166.7	158.4	164.6	162.0
AB2 [Hz]	170.7	133.3	200.3	166.9	162.9	131.4
TAB [Hz]	341.0	302.1	367.0	325.3	327.5	293.4
Variation	**MS1.25**	**MS1.26**	**MS1.27**	**MS1.28**	**MS1.29**	**MS1.30**
	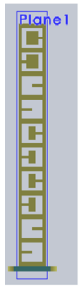	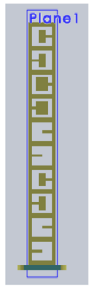	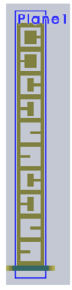	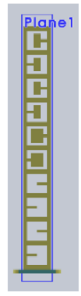	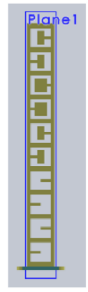	
AB1 [Hz]	157.7	158.5	162.0	160.3	156.3	153.6
AB2 [Hz]	137.1	163.4	131.4	201.1	141.9	177.1
TAB [Hz]	294.8	321.9	293.4	361.4	298.2	330.7

is a 3D printing process, whose resolution was falling within the range of 0.1 to 0.3 mm. The material used was from Acrylonitrile butadiene styrene and its characteristics are given in the previous section. Figure 4a displays photographs of both metastructures. These metastructures were subjected to base excitation in an experimental setup depicted in Fig. 4b. The drive signal is created utilizing a computer with the SCO-107 software package for sine sweep, with the acceleration amplitude of the base set to be 1g, where g is the gravitational acceleration. This signal is first directed to a LAS200 controller, afterwards transmitted to a LPA100 amplifier, and subsequently forwarded to an LDS V408 vibration shaker. The drive signal's frequency and amplitude are controlled by a lower accelerometer 4534-B with a sensitivity of 10 mV/g. The signal from this accelerometer is also forwarded to the controller for feedback purposes. Another accelerometer of identical type is attached to the centre of uppermost horizontal plane of the metastructure to capture the response in the vertical direction. This signal is linked to both the controller and the computer for further processing and analysis.

The measured AFRCs for the top point of the original metastructure MS0 and the redesigned metastructure MS1 are given in Fig. 5. Notably, these

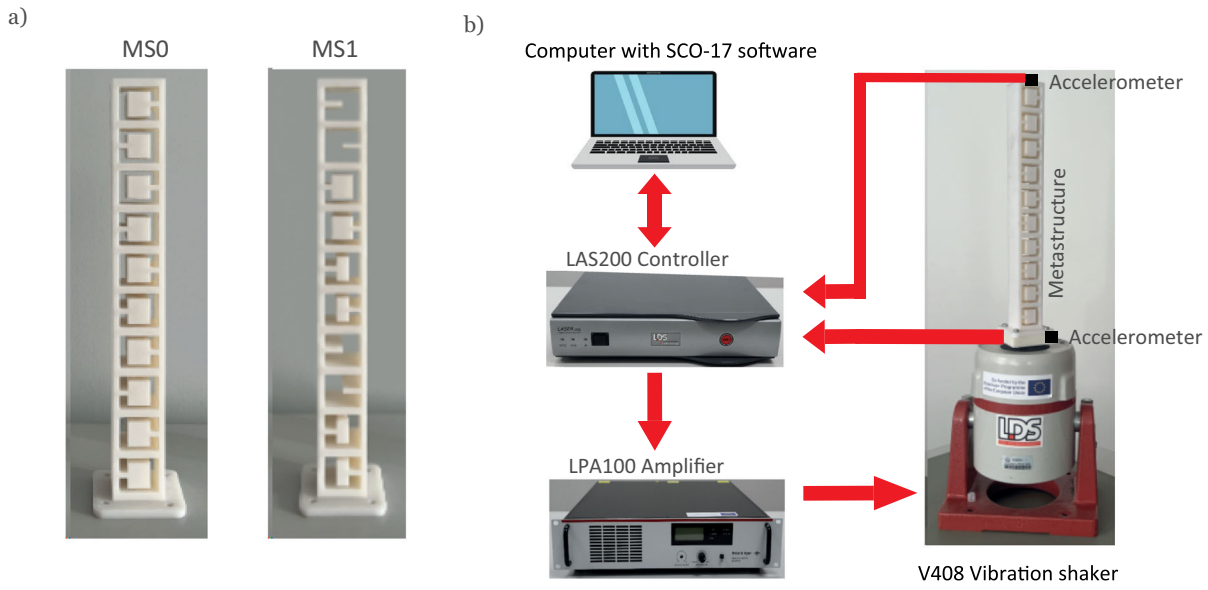

Fig. 4 **a** Fabricated metastructures: MS0 and MS1; **b** Experimental setup

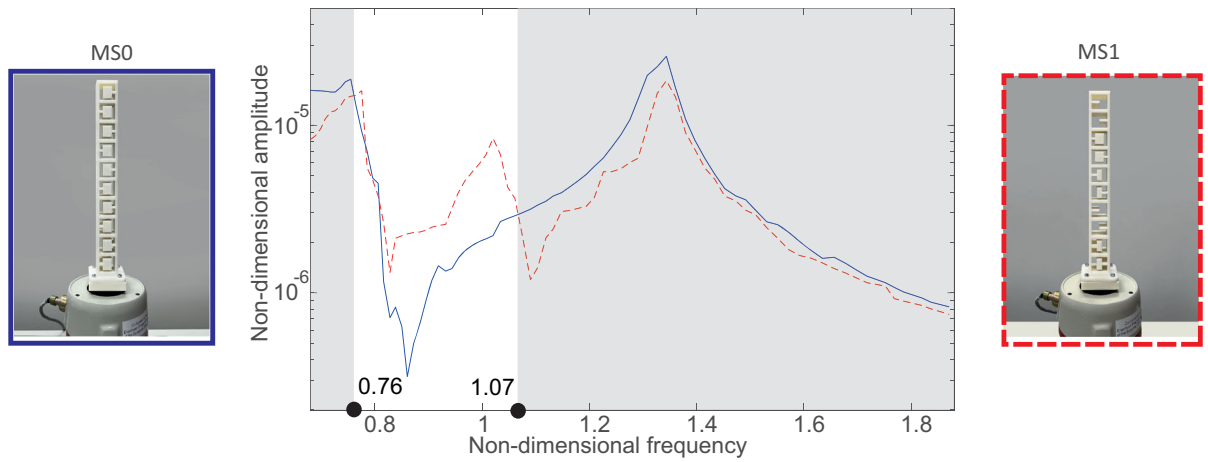

Fig. 5 Measured AFRCs of the point on the top of the redesigned metastructure MS1 compared to the original one MS0 with the attenuation region shaded in grey

responses can be qualitatively linked to the numerically obtained curves in Fig. 3, albeit with varying peak frequency and amplitude values due to the distinct visco-elastic physical properties of the actual metastructure with respect to that considered in COMSOL Multiphysics. It should be pointed out that despite the fact that a refined FEM model was utilized for the theoretical numerical predictions and a modern rig with reliable subsequent signal processing procedures were used for getting the experimental results, the authors did not go for a complete quantitative validation, but for the qualitative one only, not aiming to prove the optimality of MS1, but to show that it is better than MS0. The main reason for this choice is that the criteria used for the data-driven approach were related to the frequency range with the geometric parameters of the metastructure as the varying ones. The rest of the system's parameters, such as damping, were not considered. This certainly affects the response quantitatively, but this was not the focus herein. The amplitude reduction in a certain frequency range (so, quantitative aspects of the response), would

require a completely different criterion than in the current study, which will be addressed in future studies.

5 Analyses of the redesigned absorbers: shapes and distributions

As discussed in the Introduction, the way how the natural frequency(ies) of absorbers should be designed and distributed along metastructures has attracted the interest of researchers. In the majority of studies conducted so far, they were designed to be all equal and tuned to the frequency of the external oscillator [1–4] or to the metastructure as a whole [16, 28, 32]. However, there have been studies that provided the evidence of the benefits of using absorbers whose natural frequency changes along a span of frequencies [18, 19, 28], linearly [32, 33] or nonlinearly [32]. It is obvious that different shapes and geometry of the absorbers in the newly designed metastructures MS1 of this study vary along the metastructure, so more detailed discussion of these variations is provided subsequently.

The absorbers from MS0 (TA0) and MS1 (TA1.1, TA1.2, TA1.3) are illustrated in Fig. 6a based on their geometrical characteristics outlined in Tables 1 and 2. Following this, their modal frequencies are examined.

All absorbers possess the characteristic of having a length of the corresponding cantilever that is smaller than its width ($L < a$). In the realm of the bending vibration theory [34], this particular characteristic necessitates the avoidance of the classical Euler–Bernoulli beam theory and instead calls for the utilization of more advanced vibration theories. Among these theories, the most suitable one is the Timoshenko beam theory [34], which incorporates two deformation mechanisms: shear deformation and rotational bending effects. These additional mechanisms of deformation are introduced through the shear modulus G of the cantilever material and the radius of gyration r_g of the tip mass. In this study, this beam theory is employed to compute the first and second modal frequencies of the absorbers. For a cantilever with a tip mass, the important parameter is the ratio μ of its tip mass M and the mass of the cantilever beam m_b:

$$\mu = \frac{M}{m_b} = \frac{\rho dba}{\rho Lea}, \tag{1}$$

where ρ is the mass density, the parameter d is taken as in the ML approach: $d = 2(15 - L)$, while the rest of the parameters are defined in Fig. 1b. For the parameter values of TA0, TA1.2 and TA1.3, the value of the ratio defined by Eq. (1) changes considerably. The first and the second modal frequency ω can be calculated from the expression [35, 36]:

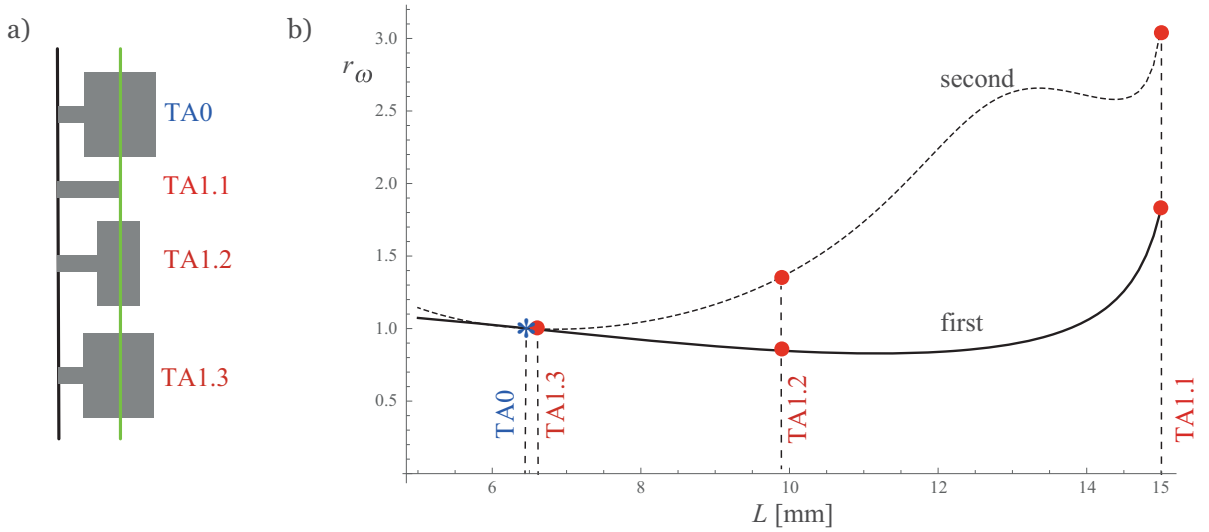

Fig. 6 **a** Sketch of the absorbers; **b** Change of the nondimensional frequency ratio r_ω for the first and second frequency, Eq. (3) with the length L

$$\omega(L) = \frac{v}{L^2}\sqrt{\frac{EIg}{A\rho}} = \frac{v}{L^2}\sqrt{\frac{Ege^2}{12\rho}}, \tag{2}$$

where E is Young's modulus of elasticity, I is the moment of inertia $I = \frac{ae^3}{12}$, g is the gravitational acceleration, A is the cross-sectional area of the beam, while v is the solution of the characteristic Eq. (4) given in Appendix [35, 36], where the existence of the aforementioned shear modulus G in the parameter s is noticeable (see Eq. (5)), alongside the Young's modulus of elasticity E. Of interest herein are the two lowest solutions of Eq. (2), i.e. Eq. (5). One can now define the nondimensional frequency ratio r_ω as the ratio of the natural frequency $\omega(L)$ given by Eq. (2) with respect to the natural frequency $\omega(L_0)$ of the absorber in MS0:

$$r_\omega = \frac{\omega(L)}{\omega(L_0)}, \tag{3}$$

where L_0 corresponds to the length L of MS0 defined in Table 1. This expression is plotted in Fig. 6b for the first and second modal frequency. Note that the following numerical values are used: $E = 2 \cdot 10^9 \frac{\mathrm{N}}{\mathrm{m}^2}, G = 1 \cdot 10^9 \frac{\mathrm{N}}{\mathrm{m}^2}, \rho = 1050 \frac{\mathrm{kg}}{\mathrm{m}^3}, g = 9.81 \frac{\mathrm{m}}{\mathrm{s}^2}$ to match the one in the previous numerical and experimental considerations.

It is seen that the nondimensional ratio r_ω changes neither monotonically not linearly with the length L. Apparently, this change is both non-monotonous and nonlinear. The values of r_ω that correspond to all TAs are depicted by red circles, while the one corresponding to TA0 is depicted by the blue asterix. Note that given Eq. (3), the values of r_ω for TA0 are equal to unity. This enables one to compare the modal frequencies of other TAs with respect to the original one TA0. What is seen is that in MS1, the ML yielded the design with the absorbers TA1.1 with both the first and second modal frequency being considerably higher than the original one, while TA1.2 and TA1.3 have the first modal frequency lower than TA0. When it comes to the second modal frequencies, TA1.2 has it higher than TA0. Their distribution in MS1 is nonuniform: the absorbers 1 and 2 are TA1.2 and have the lowest first modal frequency; the absorbers 3 and 4 are TA1.1 and have the highest first and second modal frequency; the absorbers 5 and 6 are TA1.2 and have the lowest first modal frequency; the absorbers 7 and 8 are TA1.3 and have the middle-valued first modal frequency and the lowest second one; the absorbers 9 and 10 are TA1.1 and have the highest modal frequencies considered. So, the distribution of the absorbers in pairs is original and for the first modal frequency follows the trend 'the lowest–the highest–the lowest–the middle-valued–the highest' first modal frequency, which is neither expected nor predictable based on the previous results [16, 18, 28, 32, 33]. This redesign and analysis answer the recommendation and guidelines given in [18]: 'A more sophisticated distributed mass model should be used to create a finalized design of the metastructure'. The evidence presented unequivocally shows that such sophisticated and original model has been achieved in this study by using the ML approach with nonlinear distribution of absorbers' modal frequencies, while previous analytical and numerical attempts [16, 18, 28, 32, 33] have not reached it with the same outcome. These facts support the utilization of a data-science methodology done herein.

6 Conclusions

The focus of this research has been on the redesign of integrated internal oscillators within a 10-unit-metastructure that exhibits longitudinal vibrations, in order to achieve effective vibration reduction around specific resonance frequencies—either the second one, or both the first and second one simultaneously. The original metastructure is uniform, with identical absorbers throughout. These absorbers consist of cantilevers integrated into the external units of the metastructure, each featuring a block mass at the end of a cantilever.

As the previous theoretical investigations failed to redesign this structure to achieve beneficial vibration attenuation around the second resonance, a data science approach—a machine learning technique, has been employed to redesign it so that it contains the same shape of the absorbers as the original metastructure. To assure a relatively simple manufacturing process, adjustments have been made to the length of the cantilever and the concentrated block at the tip. However, to keep the axis of the metastructure fixed and prevent bending, the total length of the cantilever and half the length of the tip mass must remain constant. This physics-based condition has been a key consideration during the redesign phase. To

further prevent bending, the second physics-based condition for variations involves redesigning internal oscillators in five pairs to achieve balanced momenta caused by their weight with respect to the point where they are attached to the external units. By addressing three variations of absorbers on these five pairs, a total of 243 different metastructures have been analysed using COMSOL Multiphysics software to generate AFRCs for each point on the top of the structures. Subsequently, a support vector regression model has been utilized to analyse the dataset and produce AFRCs for various geometrical parameters of the internal oscillators compared to those obtained in COMSOL Multiphysics. Finally, an optimization process has been conducted to determine the optimal geometry of the internal oscillators in the metastructure to achieve the widest possible attenuation region.

The achievement of the vibration mitigation around the second resonance, along with the simultaneous consideration of both the first and second resonances, has been attained using a metastructure that incorporates three distinct types of absorbers, which possess dimensions and distributions that were neither initially intuitive nor expected. The three types of absorbers in this metastructure are as follows: absorbers 3, 4, 9, and 10 resemble a cantilever-like structure with the longest length; absorbers 1, 2, 5, and 6 feature a longer cantilever and a shorter tip mass than the original absorbers; and absorbers 7 and 8 consist of a slightly longer cantilever and a slightly short tip block than the original absorbers. The redesigned metastructure has been manufactured using 3D printing technology and subsequently subjected to experimental investigation. The experiments have qualitatively validated that the newly designed metastructure exhibits better vibration attenuation capabilities compared to the original structure based on the established criteria and in the frequency region considered. Furthermore, an advanced theory on bending vibrations has been applied to analyse the modal frequencies of the vibration absorbers and their distribution across the metastructures. The nonlinear variations in these frequencies with the length of the absorbers' cantilever have been illustrated, showcasing the complexity that would have been challenging to predict analytically. This complexity underscores the importance of utilizing machine learning techniques undertaken in this work.

The strategy and workflow outlined in this research—the creation of the initial database in modelling-enabled software, and further application of ML techniques to train the metastructure model, extending the original discrete database to a continuous one, can be applied to identify the optimal design of metastructures composed of different materials and featuring various shapes and geometries for their vibration dampers, which highlights its generality and applicability.

Regarding the future work, as noted in Sect. 4.2, different optimality criteria for the redesign can be considered from the viewpoint of the vibration control purposes. Instead of observing only the width of the frequency region where the displacement amplitude is reduced, one can also take into account the total amount of the displacement amplitude reduction (so, calculate the integral and its change over a certain frequency range), and this is currently in the process of reporting by the authors. In this way, the quantitative aspect will be tackled, and not only the qualitative as it has been the case in this study. In addition, by using appropriate weighting factors in an optimality criterion, the main frequency region(s) of interest for the displacement amplitude reduction can be specified.

Author contributions I.K.: Conceptualization, Methodologies, Analytical considerations, Visualization, Writing—review & editing. Z.K.: ML models design and evaluation, Numerical optimisation, Experimental analysis and results presentation. V.R.: Production of numerical dataset and Preparation for practical realisation of experiments. Lj.T.: Concept for variations and numerical analysis. R. Z.: Interpretation of the results, Concept for validations.

Funding This study has been realised during the NOLIMAST research project funded by the Ministry of Science, Technological Development and Innovation of the Republic of Serbia. R. Zhu acknowledges and expresses gratitude to the support from the National Key R&D Program of China under Grant No. 2021YFE0110900.

Declarations

Competing interests The authors do declare that this work was conducted in the absence of any commercial or financial relationships that could be seen or treated as a potential conflict of interest.

Data availability The raw/processed data required to reproduce these findings cannot be shared at this time as the data also forms part of an ongoing study.

Appendix

For a mass-loaded clamped-free Timoshenko beam, the characteristic equation with respect to the parameter v appearing in Eq. (2) can be written down as [35, 36]:

$$\begin{aligned}&\frac{\alpha^2+s^2}{\alpha}(R_3R_8-R_7R_4+R_4R_5-R_1R_8)\\&+\frac{\beta^2-s^2}{\beta}(R_2R_7-R_6R_3+R_1R_6-R_2R_5)\\&=0,\end{aligned}\tag{4}$$

where

$$\alpha=\frac{1}{\sqrt{2}}\sqrt{-(r^2+s^2)+\sqrt{(r^2-s^2)+\frac{4}{v^2}}},$$

$$\beta=\frac{1}{\sqrt{2}}\sqrt{(r^2+s^2)+\sqrt{(r^2-s^2)+\frac{4}{v^2}}},\tag{5}$$

$$s=\frac{1}{L}\sqrt{\frac{Ee^2}{8G}},$$

$$r=\frac{e}{\sqrt{12}},$$

$$R_1=\mu v^2\cosh(v\alpha)+\frac{v}{\alpha}\sinh(v\alpha),$$

$$R_2=\mu v^2\sinh(v\alpha)+\frac{v}{\alpha}\cosh(v\alpha),$$

$$R_3=\mu v^2\cos(v\beta)+\frac{v}{\beta}\sin(v\beta),$$

$$R_4=\mu v^2\sin(v\beta)-\frac{v}{\beta}\cos(v\beta),$$

$$R_5=\frac{\alpha^2+s^2}{\alpha}\left(v\alpha\cosh(v\alpha)-\frac{1}{2}\mu\frac{r_g^2}{L^2}v^2\sinh(v\alpha)\right),$$

$$R_6=\frac{\alpha^2+s^2}{\alpha}\left(v\alpha\sinh(v\alpha)-\frac{1}{2}\mu\frac{r_g^2}{L^2}v^2\cosh(v\alpha)\right),$$

$$R_7=-\frac{\beta^2-s^2}{\beta}\left(v\beta\cos(v\beta)-\frac{1}{2}\mu\frac{r_g^2}{L^2}v^2\sin(v\beta)\right),$$

$$R_8=\frac{\beta^2-s^2}{\beta}\left(-v\beta\sin(v\beta)-\frac{1}{2}\mu\frac{r_g^2}{L^2}v^2\cos(v\beta)\right],$$

$$r_g=\sqrt{\frac{d^2+b^2}{12}}.$$

References

1. Hussein, M.I., Leamy, M.J., Ruzzene, M.: Dynamics of phononic materials and structures: historical origins, recent progress, and future outlook. Appl. Mech. Rev. **66**(4), 040802 (2014)
2. Dalela, S., Balaji, P.S., Jena, D.P.: A review on application of mechanical metamaterials for vibration control. Mech. Adv. Mat. Struct. **29**, 3237–3262 (2022)
3. Contreras, N., Zhang, X., Hao, H., Hernández, F.: Application of elastic metamaterials/meta-structures in civil engineering: a review. Compos. Struct. **28**, 117663 (2023)
4. Den Hartog, J.P.: Mechanical Vibrations. McGraw-Hill, New York (1934)
5. Rao, S.: Mechanical Vibrations, 5th edn. Prentice Hall, New York (2011)
6. Kovacic, I., Radomirovic, D.: Mechanical Vibrations: Fundamentals With Solved Examples. Willey, Hoboken (2017)
7. Gutierrez Soto, M., Adeli, H.: Tuned mass dampers. Arch. Comput. Methods Eng. **20**, 419–431 (2013)
8. Elias, S., Matsagar, V.: Research developments in vibration control of structures using passive tuned mass dampers. Annu. Rev. Control. **44**, 129–156 (2017)
9. Kela, L., Vähäoja, P.: Recent studies of adaptive tuned vibration absorbers/neutralizers. Appl. Mech. Rev. **62**(6), 1–9 (2009)
10. Lu, Z., Wang, Z., Zhou, Y., Lu, X.: Nonlinear dissipative devices in structural vibration control: a review. J. Sound Vib. **423**, 418–499 (2018)
11. Starosvetsky, Y., Gendelman, O.V.: Attractors of harmonically forced linear oscillator with attached nonlinear energy sink. II: optimization of a nonlinear vibration absorber. Nonlinear Dyn. **51**(1–2), 47–57 (2008)
12. Huang, X., Yang, B.: Towards novel energy shunt inspired vibration suppression techniques: principles, designs and applications. Mech. Syst. Signal Process. **1**(182), 109496 (2023)
13. Wang, G., Wen, X.S., Wen, J.H., Liu, Y.Z.: Quasi-one-dimensional periodic structure with locally resonant band gap. J. Appl. Mech. **73**, 1670170 (2006)
14. Frank Pai, P.: Metamaterial-based broadband elastic wave absorber. J. Intell. Mater. Syst. Struct. **21**, 517–528 (2010)
15. Xiao, Y., Wen, J., Wen, X.: Longitudinal wave band gaps in metamaterial-based elastic rods containing multi-degree-of-freedom resonators. New J. Phys. **14**(3), 033042 (2012)
16. Hobeck, J.D., Laurent, C.M.V., Inman, D.J.: 3D Printing of metastructures for passive broadband vibration suppression, In: Proceedings of the 20th international conference on composite materials, Copenhagen, 19–24 July 2015.

17. Nobrega, E.D., Gautier, F., Pelat, A., Dos Santos, J.M.C.: Vibration band gaps for elastic metamaterial rods using wave finite element method. Mech. Syst. Signal Process. **79**, 192–202 (2016)
18. Reich, K.K., Inman, D.J.: Lumped mass model of a 1D metastructure for vibration suppression with no additional mass. J. Sound Vib. **403**, 75–89 (2017)
19. Sugino, C., Xia, Y., Leadenham, S., Ruzzene, M., Erturk, A.: A general theory for bandgap estimation in locally resonant metastructures. J. Sound Vib. **405**, 104–123 (2017)
20. Lee, S., Ahn, C.H., Lee, J.W.: Vibro-acoustic metamaterial for longitudinal vibration suppression in a low frequency range. Int. J. Mech. Sci. **144**, 223–234 (2018)
21. Jin, Y.B., Zeng, S.X., Wen, Z.H., He, L.S., Li, Y., Li, Y.: Deep-subwavelength lightweight metastructures for low-frequency vibration isolation. Mater. Des. **215**, 110499 (2022)
22. Muhammad, J.K., Ogun, O.: Design and fabrication of 3D-printed composite metastructure with subwavelength and ultrawide bandgaps. New J. Phys. **25**, 053015 (2023)
23. Hong, H.S., Kim, W., Kim, W.V., Jeong, J.-M., Kim, S., Kim, S.S.: Machine learning-driven design optimization of buckling-induced quasi-zero stiffness metastructures for low-frequency vibration isolation. ACS Appl. Mat. Interfaces **16**(14), 17965–17972 (2024)
24. Chen, D.K., Li, Y.G., Gong, Y.F., Li, X.Y., Ouyang, W., Li, X.B.: Low frequency vibration isolation characteristics and intelligent design method of hull grillage metastructures. Mar. Struct. **94**, 103572 (2024)
25. Liu, C.-X., Yu, G.-L., Liu, Z., Liu, C.-X., Yu, G.-L., Liu, Z., Liu, C.-X., Yu, G.-L., Liu, Z.: Fast topology optimization of phononic crystal-based metastructures for vibration isolation by deep learning. Comput. Aided Civ. Infrastruct. Eng. **39**(5), 776–790 (2024)
26. Michaloliakos, A., Wang, C.G., Vakakis, A.F.: Machine learning extreme acoustic non-reciprocity in a linear waveguide with multiple nonlinear asymmetric gates. Nonlinear Dyn. **111**, 17277–17297 (2023)
27. He, L.S., Li, Y., Torrent, D., Zhuang, X.Y., Rabczuk, T., Jin, Y.B.: Machine learning assisted intelligent design of meta structures: a review. Microstruct. **3**, 2023037 (2023)
28. Kovacic, I., Teofanov, L.J., Kanovic, Z., Zhao, J., Zhu, R., Rajs, V.: On the influence of internal oscillators on the performance of metastructures: Modelling and tuning conditions. Mech. Syst. Signal Process. **205**, 110861 (2023)
29. Yu, H., Kim, S.: SVM Tutorial: Classification, Regression, and Ranking. In: Rozenberg, G., Back, T., Kook, J.N. (eds.) Handbook of Natural Computing, pp. 479–506. Springer, Berlin (2012)
30. Meireles, M.R.G., Almeida, P.E.M., Simoes, M.G.: A comprehensive review for industrial applicability of artificial neural networks. IEEE Trans. Indus. Electron. **50**, 585–601 (2003)
31. Bhoskar, M.T., Kulkarni, M.O.K., Kulkarni, M.N.K., Patekar, M.S.L., Kakandikar, G.M., Nandedkar, V.M.: Genetic algorithm and its applications to mechanical engineering: a review. Mater. Today Proc. **2**, 2624–2630 (2015)
32. Kovacic, I., Rakaric, Z., Kanovic, Z., Rajs, V.: Metastructure with integrated oscillators of constant, linearly and nonlinearly varying natural frequency. Front. Phys. **10**, 934998 (2022)
33. Reichl, K.K., Inman, D.J.: Constant mass metastructure with vibration absorbers of linearly varying natural frequencies. Top. Modal Anal. Test. **10**, 153–158 (2017)
34. Mei, C.H.: Mechanical Wave Vibrations: Analysis and Control. Wiley, Hoboken (2023)
35. Bruch, J.C., Jr., Mitchell, T.P.: Vibrations of a mass-loaded clamped-free Timoshenko beam. J. Sound Vib. **114**, 341–345 (1987)
36. Horr, A.M., Schmidt, L.C.: Closed-form solution for the Timoshenko beam theory using a computer-based mathematical package. Comput. Struct. **55**, 405–412 (1995)